Supporting Information

Cryptic Oxidative Transamination of Hydroxynaphthoquinone in Natural Product Biosynthesis

Tomohiro Noguchi,[1,†] Shota Isogai,[1,†] Tohru Terada,[1,2] Makoto Nishiyama,[1,2] and Tomohisa Kuzuyama[1,2,*]

[1]Graduate School of Agricultural and Life Sciences and [2]Collaborative Research Institute for Innovative Microbiology, The University of Tokyo, 1-1-1 Yayoi, Bunkyo-ku, Tokyo 113-8657, JAPAN, [†]Equal contribution, *utkuz@g.ecc.u-tokyo.ac.jp

Contents

Experimental Section

Chemicals

All chemicals including standard pyridoxal 5'-phosphate (PLP) were purchased from Sigma-Aldrich unless otherwise described. Flaviolin, mompain, and 8-AF were purified in our previous work[1].

Bacterial strains and vectors

Escherichia coli DH5α was used for plasmid cloning. *E. coli* BL21 (DE3) and M15 were used for expressing recombinant proteins. *Streptomyces albus* G153 was used as a heterologous host. The pT7Blue T-vector (Novagen) was used for cloning PCR products. pQE30 (QIAGEN), and pACYCduet (Novagen) were used for protein expression. A *Streptomyces-E. coli* shuttle vector, pSE101[2], was used for heterologous expression.

Heterologous expression of *nphCDE* in *Streptomyces albus* G153

The genome of *Streptomyces* sp. strain CL190 was used as a PCR template for ligation into the *Streptomyces-E. coli* shuttle vector pSE101. The accession number of the nucleotide sequences for *nphCDE* is AB564747 in DDBJ/EMBL/GenBank nucleotide sequence database.[1] PCR amplification was performed using the forward primer pSNT-N and the reverse primer pSNT-C1 (Table 1). Because the genes cloned downstream of the *lac* promoter in pSE101 are efficiently expressed in *Streptomyces albus* G153[1], the amplified *Xba*I–*Hin*dIII fragment was blunted by DNA blunting kit (Takara) and cloned into immediately downstream of the *lac* promoter of pSE101, resulting in pSNT1 (containing NphC and NphD). The construction of pSNT2 (containing NphC, NphD, and NphE) was accomplished using the forward primer pSNT-N and the reverse primer pSNT-C2 (Table 1) in the same manner as for pSNT1. The transformation of *S. albus* G153 was performed using the protoplast method. The *S. albus*/pSNT1 and *S. albus*/pSNT2 were precultured for 2 days at 30 °C in tryptone soya broth medium (Kanto Chemical) with 25 μg mL^{-1} thiostrepton. One hundred mL of NMMP medium containing 10 μg mL^{-1} thiostrepton in a 500-mL Erlenmeyer flask was then inoculated with 2 mL of pre-culture and cultivated for 5 days at 27 °C. The supernatants of the cultures were then extracted with ethyl acetate. The products in the extract were analyzed on an HPLC system equipped with an MD-2010 Plus Photodiode array (JASCO, Tokyo, Japan) and a PEGASIL ODS column (4.6 ϕ × 250 mm; Senshu Scientific, Tokyo, Japan) under the following conditions: mobile phase A, Methanol + 0.1% trifluoroacetic acid (TFA); mobile phase B, water + 0.1% TFA; 40% to 60% A over 30 min, 100% A for 10 min, 40% A for 20 min; flow rate, 0.8 mL min^{-1}.

Inactivation of the gene *nphE*

The disruption of *nphE* was achieved by inserting a *Spe*I linker into *nphE*, resulting in plasmid pUNT5. The resulting plasmid pUNT5 was introduced into *Streptomyces* sp. strain CL190 (wild-type, CL190/wt) by the protoplast method. Double-crossover mutants were selected by PCR analysis. The PCR fragment of the gene replacement disruptant (CL190/*dnphE*) was digested by *Spe*I, whereas that of the wild-type not.

Conversion of 8-AF to naphterpin

The CL190/*dnphE* disruptant was grown in NMMP medium at 27 °C. After 2 days, 0.2 mg of 8-AF was added to the 10 mL culture and further cultivated for 3 days. The broth (10 mL) was extracted with the same volume of ethyl acetate. The organic phase was evaporated, and the residue was dissolved in methanol. The resultant methanol solution was analyzed on LC-MS/MS system equipped with a Capcell Pak C_{18} IF2 column (2.0 ϕ × 50 mm; column temperature, 40 °C; Shiseido). Analysis was carried out at a flow rate of 0.4 mL min^{-1} with a linear gradient from 10% to 90% B over 4 min, 90% B for 1 min, and then 10% for 5 min (solvent A: water + 0.1% formate; solvent B: acetonitrile + 0.1% formate). A high-resolution MS apparatus (API 3000) was used to monitor metabolites. The MS and MS/MS were performed by ESI in the negative ion mode.

Expression and purification of N-terminal His-tagged proteins

For the construction of the expression plasmids pACYC_*nphE* (*nphE* in pACYCduet), the *nphE* genes were amplified from the genomic DNA of *Streptomyces* sp. strain CL190 using the primers as listed in Table 1. *E. coli* BL21 (DE3) harboring pACYC_*nphE* were cultivated in 500 mL of liquid TB medium containing appropriate antibiotics and grown at 37 °C to an A_{600} of 1.5. The cells were cooled on ice for 10 min and isopropyl thiogalactoside was added to a final concentration of 0.5 mM. After 20 h of cultivation at 18 °C, the cells were harvested by centrifugation and resuspended in 50 mL of lysis buffer (50 mM Tris-HCl (pH8.0), 500 mM NaCl, 20% (w/v) Glycerol, 20 mM imidazole, and 1% Tween20). The cell suspension was sonicated with a Branson Sonifier (Emerson Japan, Tokyo, Japan) and then centrifuged for 20 min at 17,000 rpm at 4 °C. The supernatant was applied to a Ni-nitrilotriacetic acid-agarose column (Qiagen, Tokyo, Japan) and the recombinant protein was eluted with 250 mM imidazole in 50 mM Tris-HCl (pH8.0), 500 mM NaCl, and 20% (w/v) Glycerol. The purified recombinant NphE was dialyzed 50 mM Tris-HCl (pH8.0) and 100 mM NaCl. All recombinant proteins were concentrated by centrifugation using Viva spin (Sartorious) at 4 °C. Gel filtration was performed for purified N-terminal His-tagged NphE (expressed with pHis8[3]) NphE was dialyzed overnight in 20 mM Tris-HCl, pH 8.0 containing 150 mM NaCl, 50 μM PLP, and 2 mM L-Glu while His-tag cleavage was performed with thrombin. The dialyzed proteins were applied

to a HiLoad 26/60 Superdex 200 column (GE Healthcare, Tokyo, Japan) equilibrated with 20 mM Tris-HCl, pH 8.0 containing 150 mM NaCl, 50 μM PLP, and 2 mM L-Glu.

Assay for aminotransferase activity of NphE

To determine the amine donor of NphE, the NphE assay was performed with 20 kinds of L-amino acids as an amine donor. The reaction mixture (200 μL) contained 100 mM HEPES-NaOH (pH7.5), 50 μM mompain, 2 mM L-amino acid, 50 μM PLP, and 20 μM NphE. After incubation of the assay for 1 h at 30 °C, the reaction was stopped by adding 200 μL of methanol. The resulting mixture was centrifuged at 15,000 rpm for 10 min to remove protein. Then, the supernatants were analyzed on a HPLC system equipped with an MD-2010 Plus Photodiode array (JASCO, Tokyo, Japan) and a CAPCELL PAK C18 Mg II column (4.6 ϕ × 250 mm; OSAKA SODA, OSAKA, Japan) under the following conditions: mobile phase , 45%Methanol + 0.1% trifluoroacetic acid (TFA); for 30 min; flow rate, 1.0 mL min^{-1}. The assay using NphE mutants was performed in 100 mM HEPES-NaOH (pH7.5), 50 μM mompain, 5 mM L-amino acid, 50 μM PLP, and 2 μM NphE. After incubation of the assay for 1 h at 30 °C, the reaction was stopped by adding 200 μL of methanol. The resulting mixture was centrifuged at 15,000 rpm for 10 min to remove protein. The supernatant was analyzed by HPLC which was carried out as described above. The assay using flaviolin or mompain as an amino acceptor was performed in 100mM HEPES-NaOH (pH7.5), 50 μM flaviolin, 5 mM L-glutamate, 50 μM PLP, 0.5 mg ml^{-1} NphE in a total volume of 200 μL. The reaction mixture was incubated for 1 h at 30 ^{o}C and then terminated by addition of 200 μL of methanol. The resulting mixture was centrifuged at 15,000 rpm for 10 min to remove protein. The supernatants were analyzed on a HPLC system equipped with an MD-2010 Plus Photodiode array (JASCO, Tokyo, Japan) and a PEGASIL ODS column (4.6 ϕ × 250 mm; Senshu Scientific, Tokyo, Japan) under the following conditions: mobile phase A, Methanol + 0.1% trifluoroacetic acid (TFA); mobile phase B, water + 0.1% TFA; 40% to 60% A over 30 min, 100% A for 10 min, 40% A for 20 min; flow rate, 0.8 mL min^{-1}.

UV-Vis analysis of NphE

The UV-Vis analysis was performed with UV-1900i (Shimadzu). The NphE reaction for the UV-Vis analysis was performed in the reaction mixture containing 100 mM HEPES-NaOH (pH7.5), 50 μM mompain, 10 mM L-glutamate, and 40 μM NphE in a total volume of 500 μL. For the microaerobic condition, the reaction mixture was exposed to Ar gas for 1 h to eliminate O_2. The reaction mixture was incubated for 30 min at 25 °C.

O_2 consumption analysis of NphE

The NphE reaction was pursued by oxygen consumption using a Clark-type electrode coupled with computer integration OXYT1+R Oxygraph electrode control unit (Hansatech). The NphE reaction was performed in the reaction mixture containing 100 mM HEPES-NaOH (pH7.5), 100 μM mompain, 50 μM PLP, 10 mM L-glutamate, and 20 μM NphE in a total volume of 1 mL in the absence or presence of 0.1 mg/mL Catalase (Sigma). The reaction mixture was incubated for 10 min at 25 °C and then terminated by the addition of an equal amount of methanol. The amount of 8-AF was measured by HPLC.

Calculation of UV-Vis absorption

Firefly QC package[4], which is partially based on the GAMESS (US)[5] source code, was used for the optimization of structures, frequency calculation, and UV-Vis estimation based on the time-dependent density-functional theory (TDDFT). The B3LYP functional and the 6–31G (d) basis set were used with consideration of the solvation effect of water. A phosphate group of the PMP-mompain adduct was replaced by a methyl group as was in the previous work.[6]

Steady-state kinetics of NphE

NphE kinetic assays were performed in 100 mM HEPES-NaOH (pH7.5), 50 μM PLP, mompain, and L-glutamate in a total volume of 600 μL. When the concentration of L-glutamate was kept at 100 μM, the concentrations of mompain were varied (0.5 – 6 μM). After the reaction mixture devoid of the enzyme was incubated for 3 min at 30 °C, the reaction was initiated by adding 2.73 μg of NphE and continued for 15 s. The reaction was stopped with an equal volume of ethyl acetate. The reaction mixture was adjusted to pH 3 with 65 μL of 1 M HCl, and then extracted with 600 μL of ethyl acetate twice. The organic phase was evaporated and the residue was dissolved in 50 μL of methanol. The resultant methanol solutions were analyzed by LC-MS/MS using a Capcell PAK C_{18} IFS2 column (2.0 ϕ × 50 mm; column temperature 40 °C; Shiseido). Analysis was carried out at a flow rate of 0.36 mL min^{-1} with an isocratic elution of 75% methanol + 0.1% acetate. The amount of product was calculated from a standard curve, which was obtained from LC-MS/MS fragmentation analysis using the multiple-reaction monitoring (MRM) mode. The peak area of a characteristic product ion (*m/z* 220.025) resulting from the precursor ion corresponding to 8-AF (*m/z* 220.025) was used for quantification. Steady-state kinetic parameters were calculated using the Sigmaplot 12.3 and Enzyme Kinetics Module software (Systant Software, Point Richmond, CA, USA).

Complex structure modeling and MD simulation

A model of the homodimer structure of the NphE-PMP-mompain adduct complex was constructed as follows. A model of the monomer structure of NphE was predicted by AlphaFold version 2[7]. It was then superimposed on each chain of the homodimer structure of ArnB (PDB ID: 4OCA) with PyMOL 2.4.0,[8] to generate a model of the homodimer structure of NphE. The pyridine ring of a model of the PMP-mompain adduct was also superimposed on that of the pyridoxal moiety of the ligand of ArnB. Dihedral angles of rotatable bonds of the PMP-mompain adduct were manually adjusted so that the molecule was well accommodated in the substrate-binding pocket of the NphE model.

Partial atomic charges of the PMP-mompain adduct were determined as follows. The phosphate group was removed from the model of the PMP-mompain adduct and its structure was optimized at the HF/6-31G(d) level using Gaussian 16 B.01.[9] The electrostatic potential (ESP) around the molecule was calculated at the same level and the atomic charges that fit the ESP were calculated with the restrained electrostatic potential (RESP) method using the Antechamber module[10] of the AmberTools21[11]. Atomic charges of methyl phosphate were determined in a similar manner. A topology file of the whole structure of the PMP-mompain adduct was generated using the Antechamber module. The atomic charges of the topology file were replaced with those calculated for the PMP-mompain adduct without the phosphate group, except for those of the 5′-methylene and the phosphate group of the PLP moiety, for which the atomic charges calculated for the methyl phosphate were used. The atomic charges of the 5′-methylene group of the PLP moiety were slightly modified to give an integer net charge.

The homo-dimeric complex structure was immersed in a cubic box of water, ensuring the minimum distance of 10 Å between any box face and any protein atom. Potassium ions were added so that the net charge of the system was zero. The ff14SB force field[12] was used for the proteins and the ions, the general AMBER force field 2 (GAFF2)[13] was used for the ligand, and the TIP3P model[14] was used for water. After energy minimization and equilibration, a production MD run was performed for 100 ns. During the MD simulation, the temperature was kept at 300 K using the velocity-rescaling method[15], and the pressure was kept at 1.0×10^5 Pa using the Berendsen weak coupling method[16]. Bond lengths involving hydrogen atoms were constrained using the LINCS algorithm[17,18] to allow a time step of 2 fs. Electrostatic interactions were calculated with the particle mesh Ewald method[19,20]. All MD simulations were performed with Gromacs 2021,[21] with coordinates recorded every 10 ps.

Supplementary Tables

Table S1. List of primers used in this study.

Primer	Oligonucleotide sequence (5' to 3')	Restriction site
pSNT-N	GGGTCTAGACCGTCTCACTGCCTTGCCGTCG	*Xba*I
pSNT-C1	GGGAAGCTTTCACGTCCCGCTCCGCTCGTTCG	*Hind*III
pSNT-C2	GGGAAGCTTTCATGCCGCCCCTCCCAGGGCTC	*Hind*III
pNphE_N	GGGGGATCCCGAACCCATTCCCCTGGTC	*Bam*HI
pNphE_C	GGGGAATTCTCATGCCGCCCCTCCCAGGGC	*Eco*RI

Restriction enzyme sites are underlined.

Table S2. The average probability of amino acid residues being present within 3.5 Å of the PMP-mompain adduct in chain B

Amino acid residue	Probability (%)
057B	88.27
058B	84.66
154B	99.65
178B	99.97
235A	99.72
237A	97.31
Average	94.93

Supplementary Figures

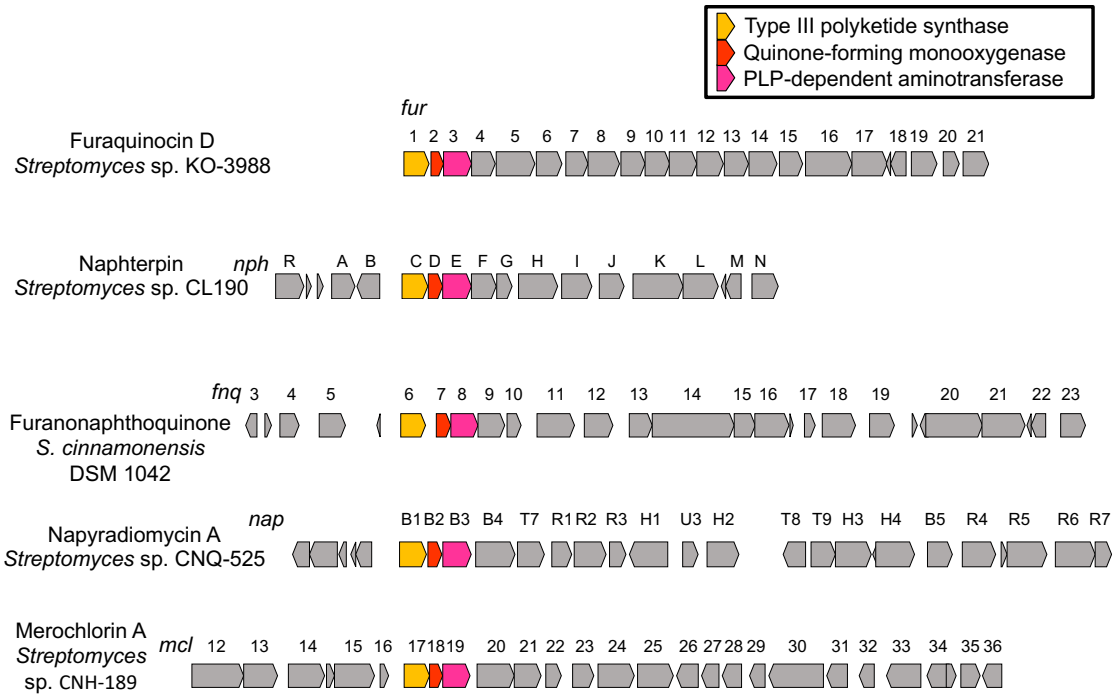

Figure S1. A conserved cassette among the biosynthetic cluster of THN-derived meroterpenoids. Three contiguous genes, *fur1*, *fur2*, and *fur3*, which encode THN synthase, monooxygenase, and aminotransferase, respectively. Homologs of these three genes are conserved among the biosynthetic clusters for THN-derived meroterpenoids.

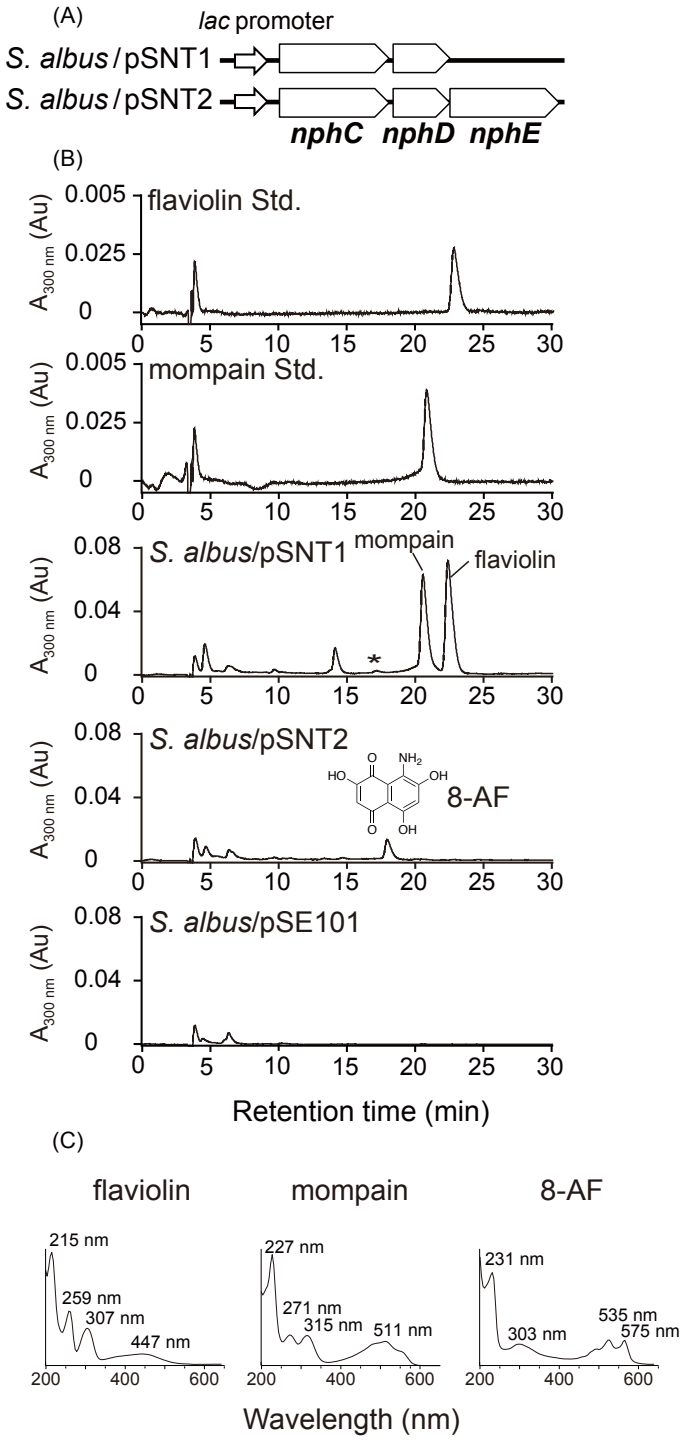

Figure S2. Heterologous expression of the *nphCDE* genes in *S. albus*. Heterologous expression of the *nph* genes in *S. albus* **(A)** Plasmid for the heterologous expression of the *nph* genes. The functions of the *nphC*, *nphD*, and *nphE* genes products were deduced as THN synthase, monooxygenase, and aminotransferase, respectively. **(B)** HPLC analysis of the ethyl acetate extracts from the broth of *S. albus* transformants. *S. albus*/pSE101 was a negative control. A negligible small peak (*) at 17 min displayed a UV-visible spectrum that was distinctly different from that of 8-amino-flaviolin. **(C)** UV-Vis spectra of standard compounds of flaviolin, momapin, and 8-AF.

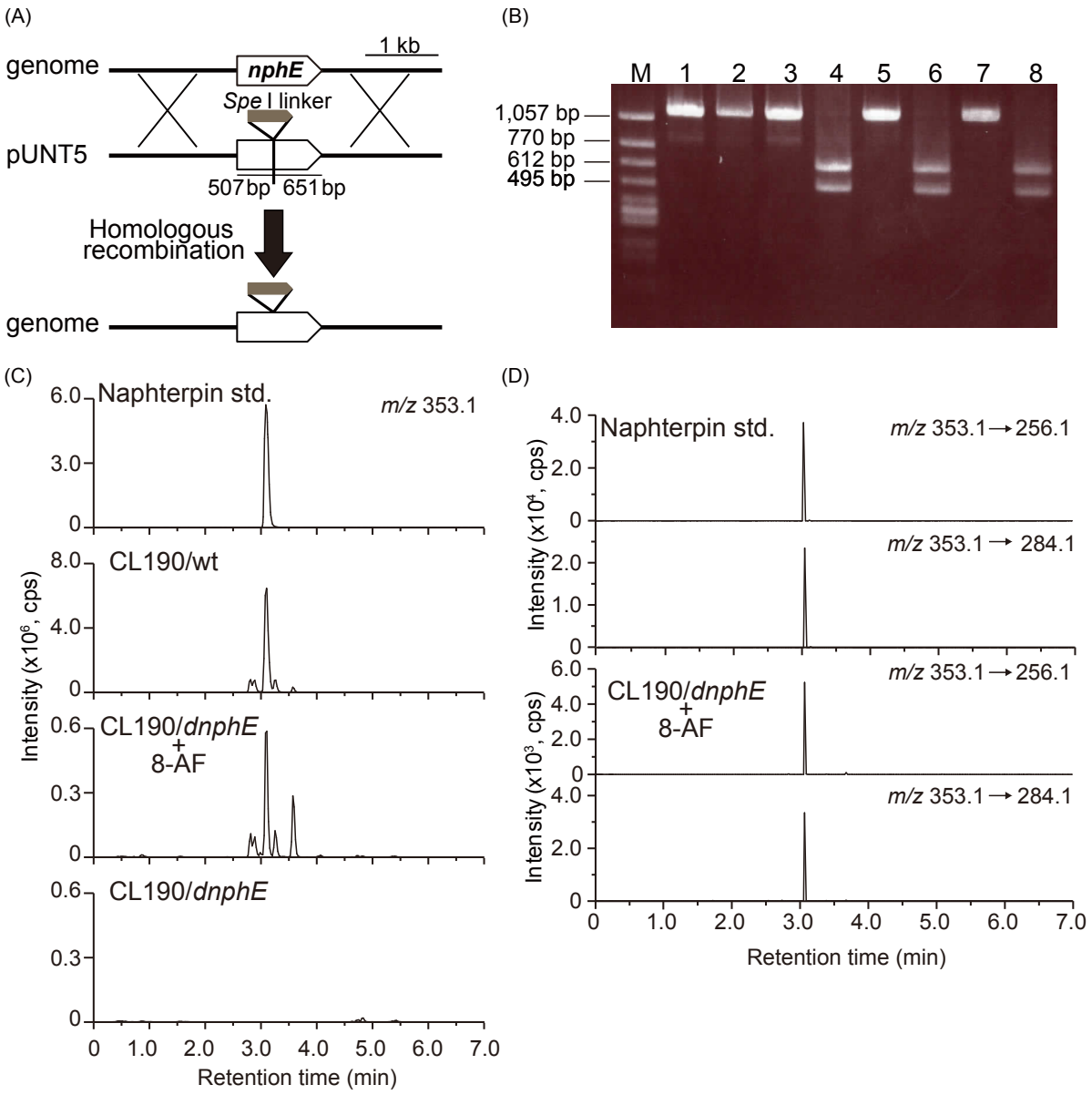

Figure S3. The *nphE* gene disruption and complement experiment. (A) The disruption method of NphE. The disruption of *nphE* was achieved by homologous recombination with a *Spe*I linker inserted *nphE* on pUNT5. **(B)** Colony PCR of the CL190 WT (Lanes 1 and 2) and the disruptants (Lanes 3–8). Amplified DNAs were examined by Spe I digestion (Lanes 2, 4, 6, and 8). M, DNA molecular marker. **(C)** Extracted ion count chromatograms of the ethyl acetate extracts from the broth of the CL190 WT and Δ*nphE*. (D) Production of naphterpin was confirmed by HPLC-MS/MS using the combinations of *m/z* 351.1/256.1 and *m/z* 353.1/284.1 in the multiple-reaction monitoring (MRM) mode.

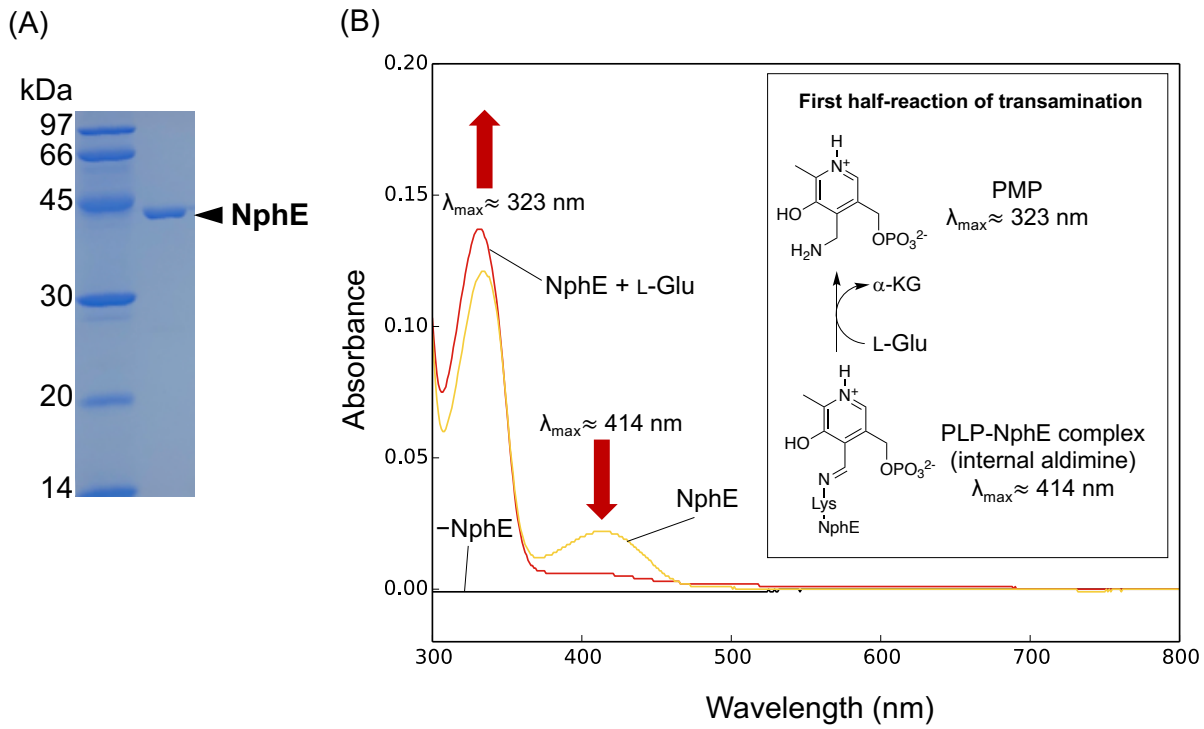

Figure S4. PMP formation with NphE and L-Glu. (A) SDS-PAGE analysis of NphE. Molecular weight of NphE is 41 kDa. **(B)** UV-Vis spectrum of the reaction mixture of 20 μM NphE. Most of NphE immediately after purification was present as the PMP (λ_{max}≈ 323 nm) bound form (yellow line). After incubation of NphE with L-Glu, the internal aldimine, (λ_{max}≈ 414 nm) was abolished and PMP bound form of NphE further increased. The first half-reaction of transamination is inserted.

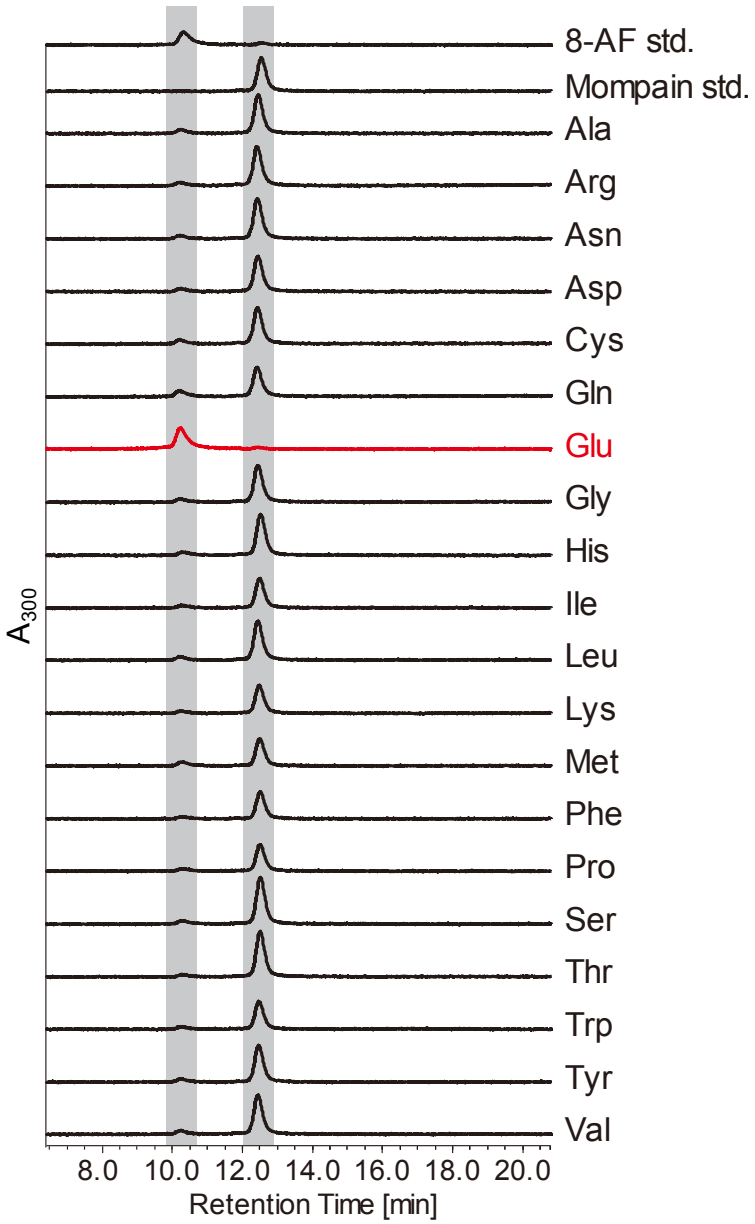

Figure S5. Examination of the amine donor of NphE. Twenty amino acids were examined as an amine donor of NphE. All of the mompain was consumed and 8-AF was produced when L-Glu was tested as an amine donor. A small amount of 8-AF was also detected when other amino acids were used, but mompain was barely consumed. This was because the majority of the recombinant NphE purified from *E. coli* contained PMP rather than a PLP-NphE complex due to intracellular L-Glu (Figure S4B).

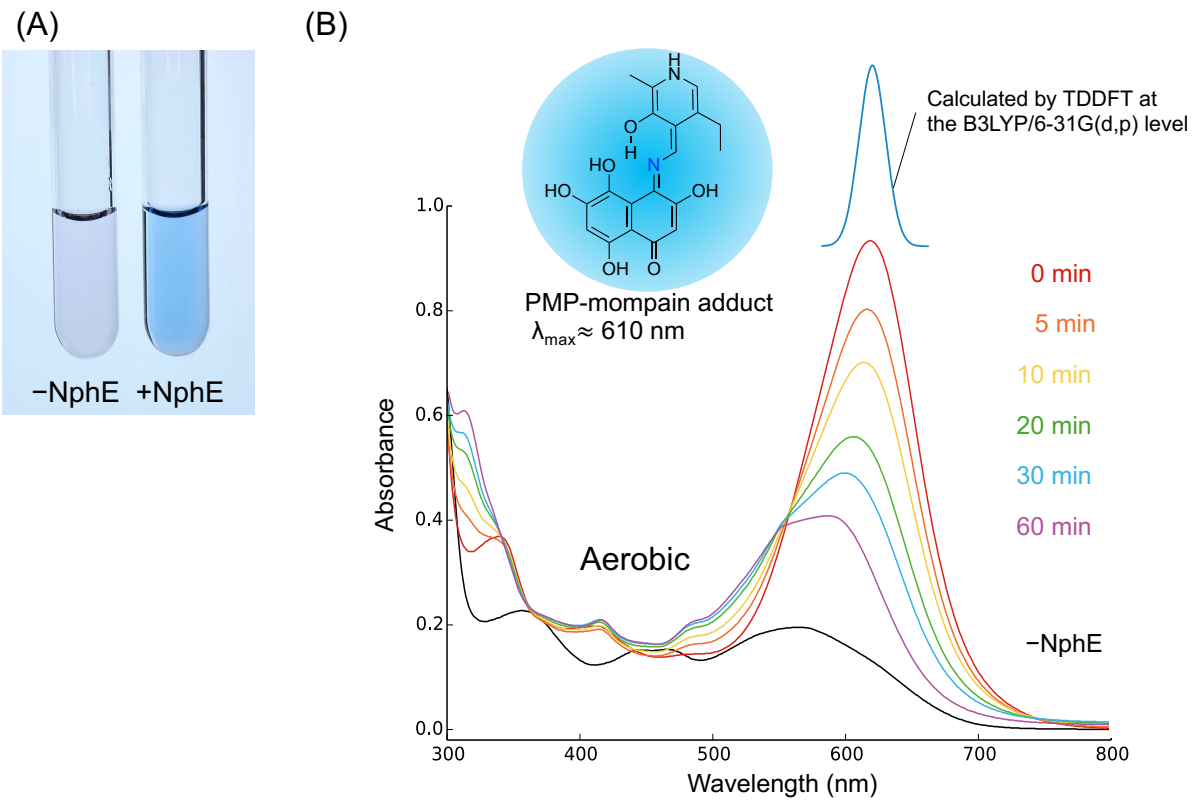

Figure S6. Monitoring of the PMP-mompain adduct during the NphE reaction. (A) The reaction mixture (*left*, –NphE) shows pink that is color of mompain. The reaction mixture (*right*, +NphE) immediately turned blue when NphE was added to the left reaction mixture. **(B)** Calculated spectrum of the PMP-mompain adduct (Quinonoid intermediate) by TDDFT (the top blue line) matches the observed spectra. The peak at 610 nm derived from the PMP-mompain adduct gradually decreased after NphE addition. In a 60 min reaction, almost all the substrate, mompain, was consumed and converted to 8-AF.

(A)

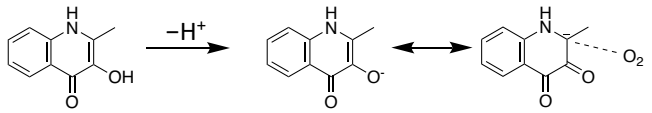

Carbanionic intermediate

(B)

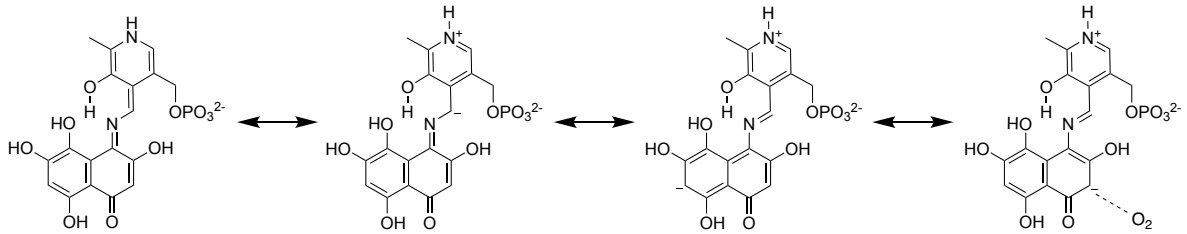

PMP-mompain adduct
(Quinonoid intermediate)

Figure S7. Carbanionic intermediates in the enzymes that react with O_2. (A) The carbanionic intermediate for cofactor-free dioxygenase, HOD. The carbanionic intermediate has a resonance structure[22]. **(B)** The PMP-mompain adduct is the carbanionic intermediate (Quinonoid intermediate) for NphE. This quinonoid intermediate has multiple resonance structures.

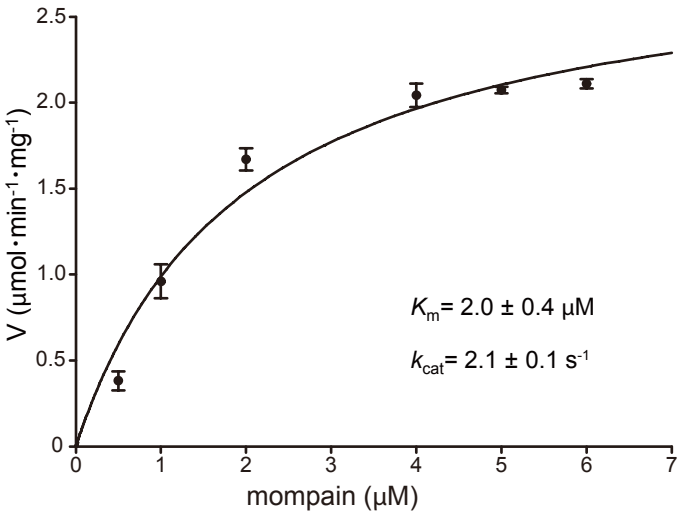

Figure S8. Kinetic analysis of NphE. The concentration of L-glutamate was fixed at 100 μM. A detailed method for the reactions was in **Experimental section**. Single-substrate kinetics with respect to varied L-Glu could not be performed due to the lack of mompain.

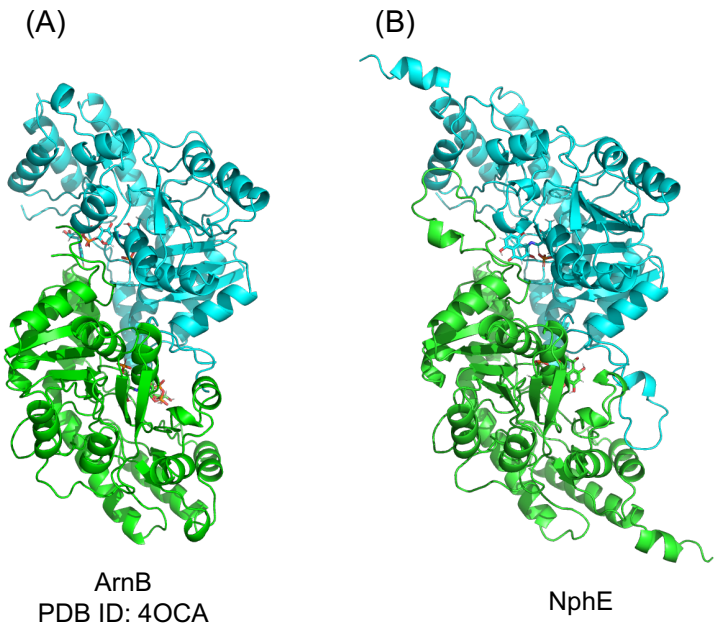

Figure S9. The predicted structure of NphE by AlphaFold v2.0. (A) The homodimeric structure of ArnB (33% identities with NphE). Chain A is colored by green and chain B is colored by cyan. **(B)** The predicted homodimeric structure of NphE by AlphFold v2.0. Chain A is colored by green and chain B is colored by cyan. Overall structure of NphE is similar to that of ArnB.

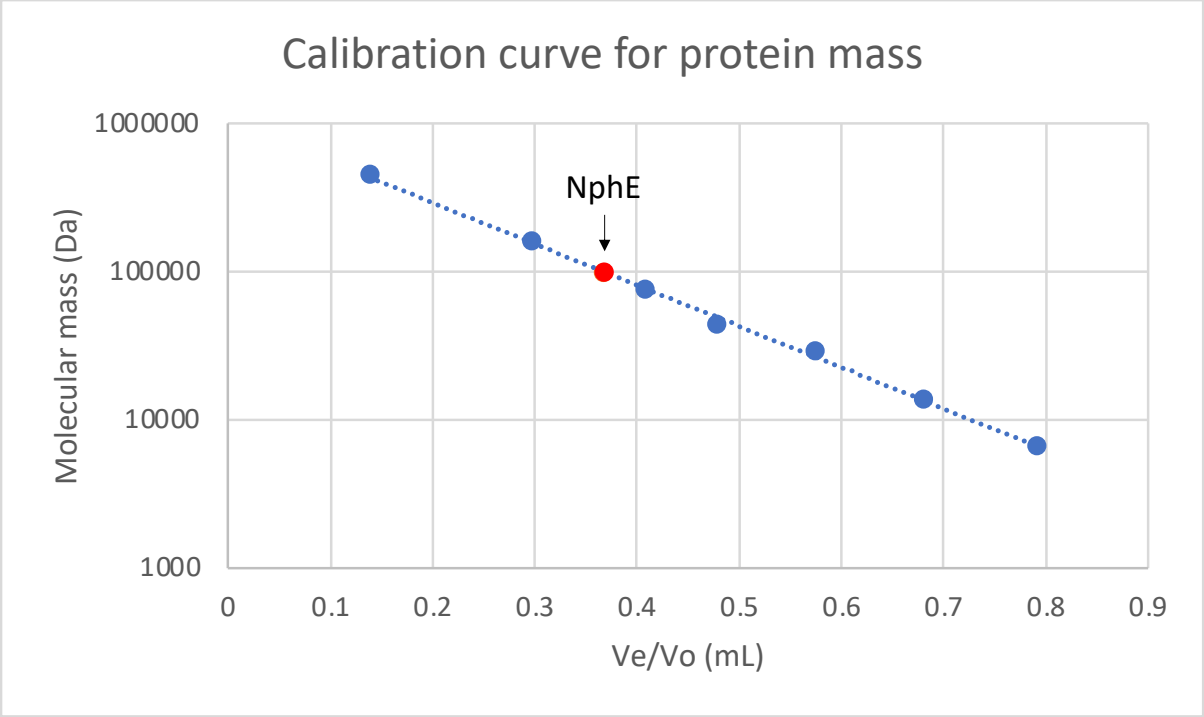

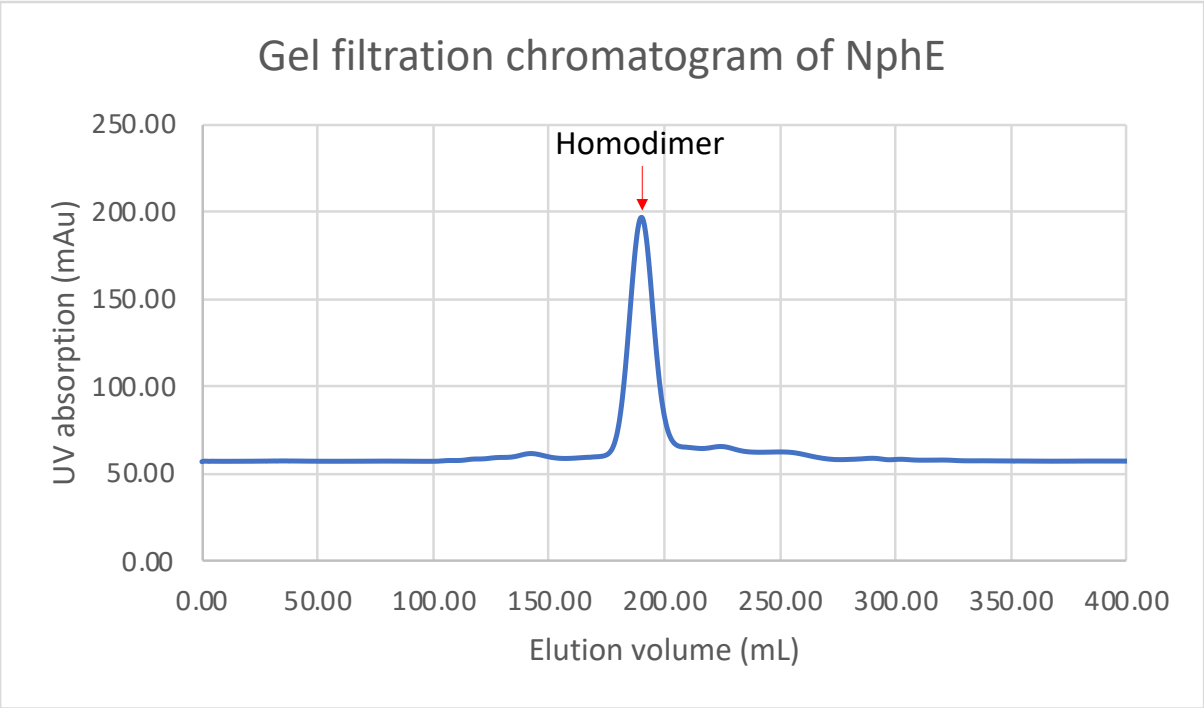

Figure S10. The gel filtration chromatogram of NphE. The theoretical molecular mass of the NphE monomer is 41 kDa and the calculated molecular mass from the gel filtration chromatogram and the calibration curve for protein mass was 96 kDa. Therefore, NphE formed homodimer in buffer. Proteins used for the calibration curve was listed as follows: Aprotinin (6500 Da), Ribonuclease A (13700 Da), Carbonic anhydrase (29000 Da), Ovalbumin (44000 Da), Conalbumin (75000 Da), Aldolase (158000 Da), Ferritin (440000 Da)

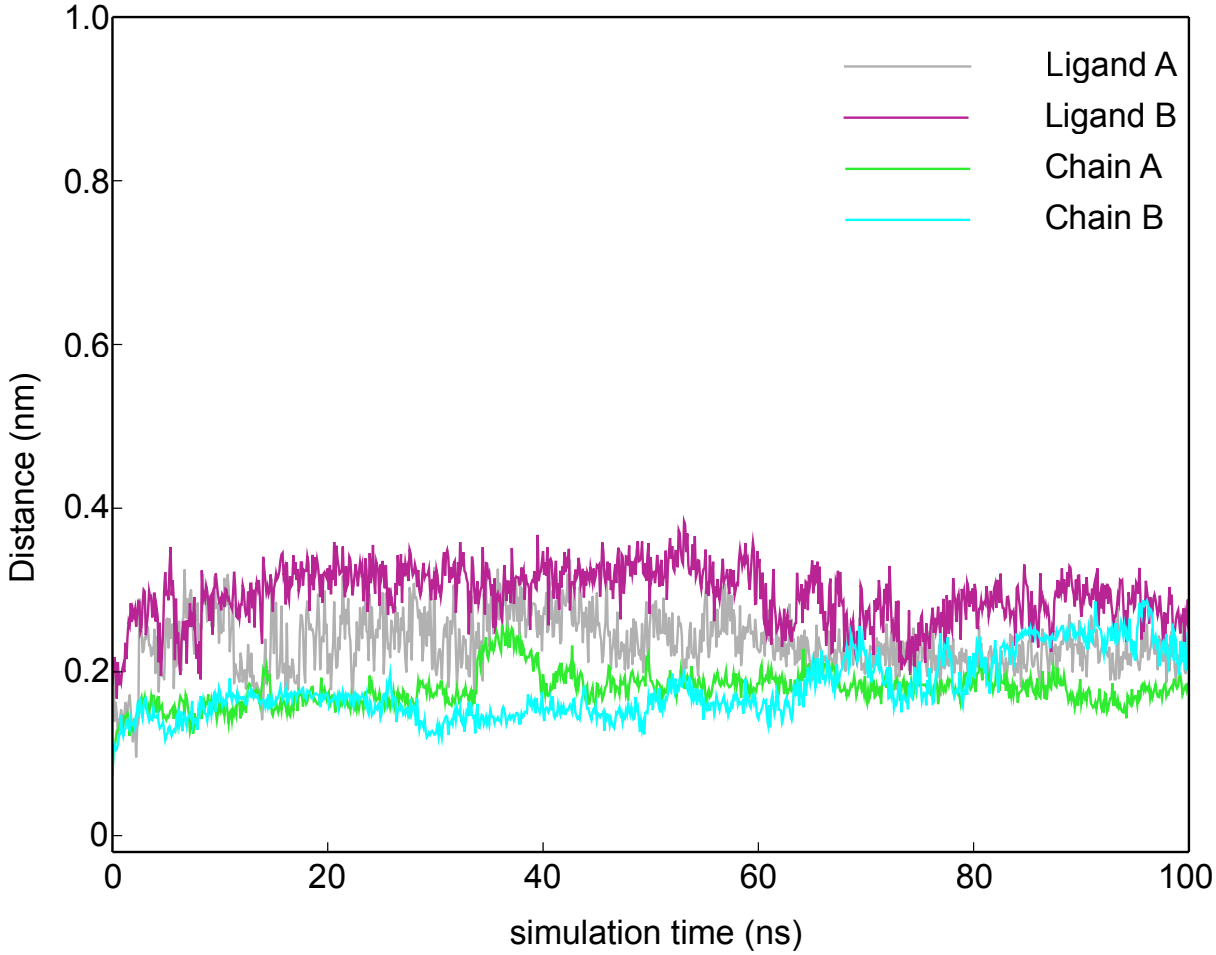

Figure S11. MD trajectories of the ligand and chains A and B. RMSD values compared to the initial structure of MD simulation. Each line shows ligand (the PMP-mompain adduct) in chain A or B, and chain A or B of NphE.

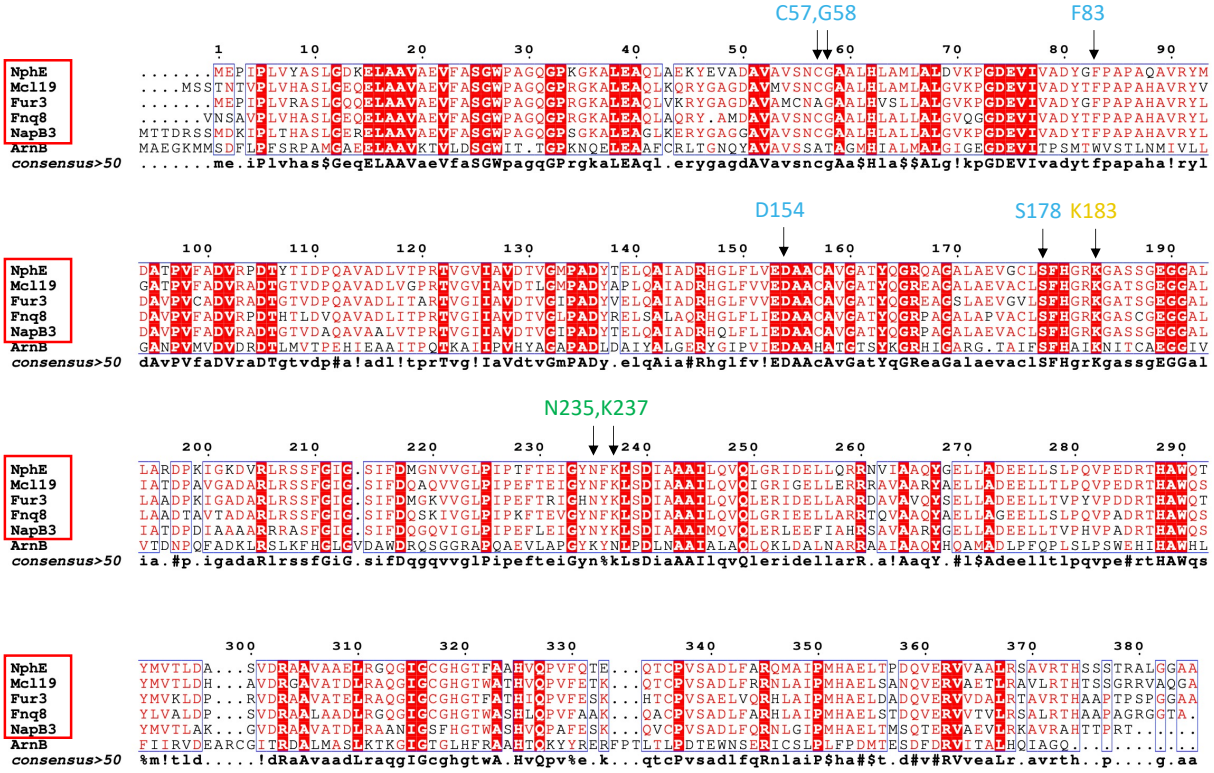

Figure S12. Conserved residues among PLP-dependent aminotransferases. Mcl19, Fur3, Fnq8, and NapB3 are NphE homologs in the biosynthetic gene clusters (BGCs) for merochlorin, furaquinocin, furanonaphthoquinone, and napyradiomycin, respectively.

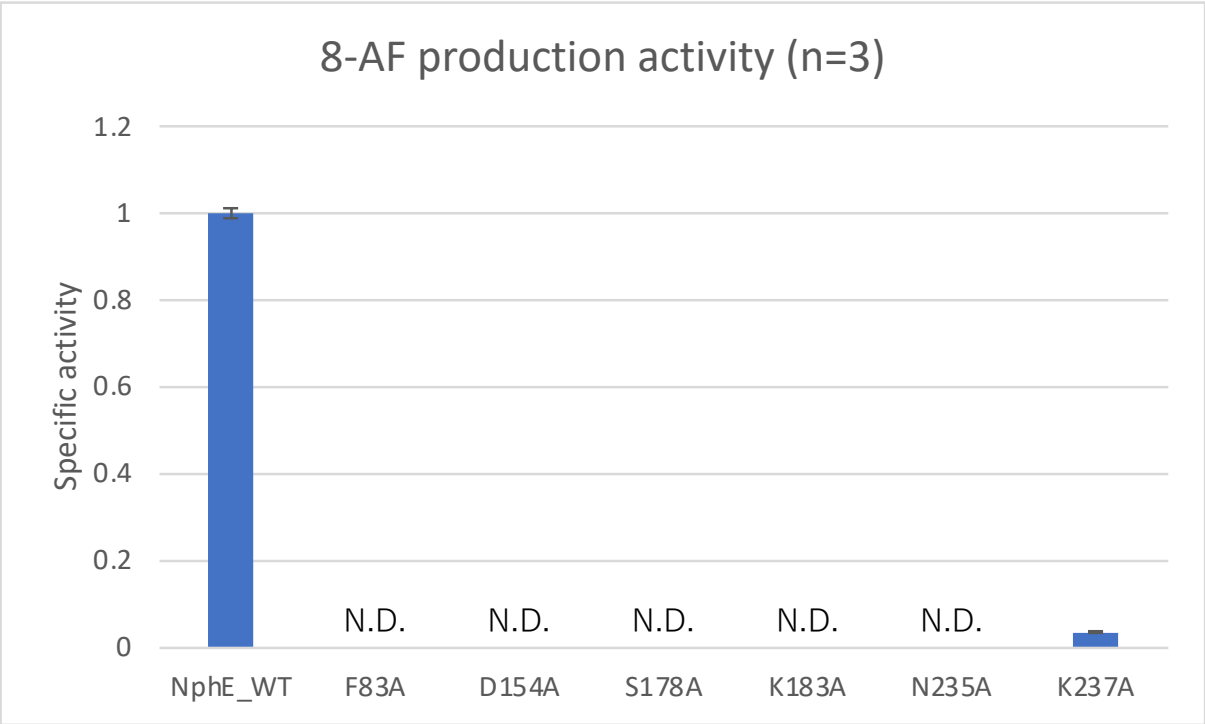

Figure S13. 8-AF production activity of the NphE mutants. The amino acid residues around PMP-mompain adduct were replaced with alanine. All mutants lost or reduced the 8-AF production activity. 8-AF production activity of the mutants were normalized by the activity of wild-type NphE (NphE_WT).

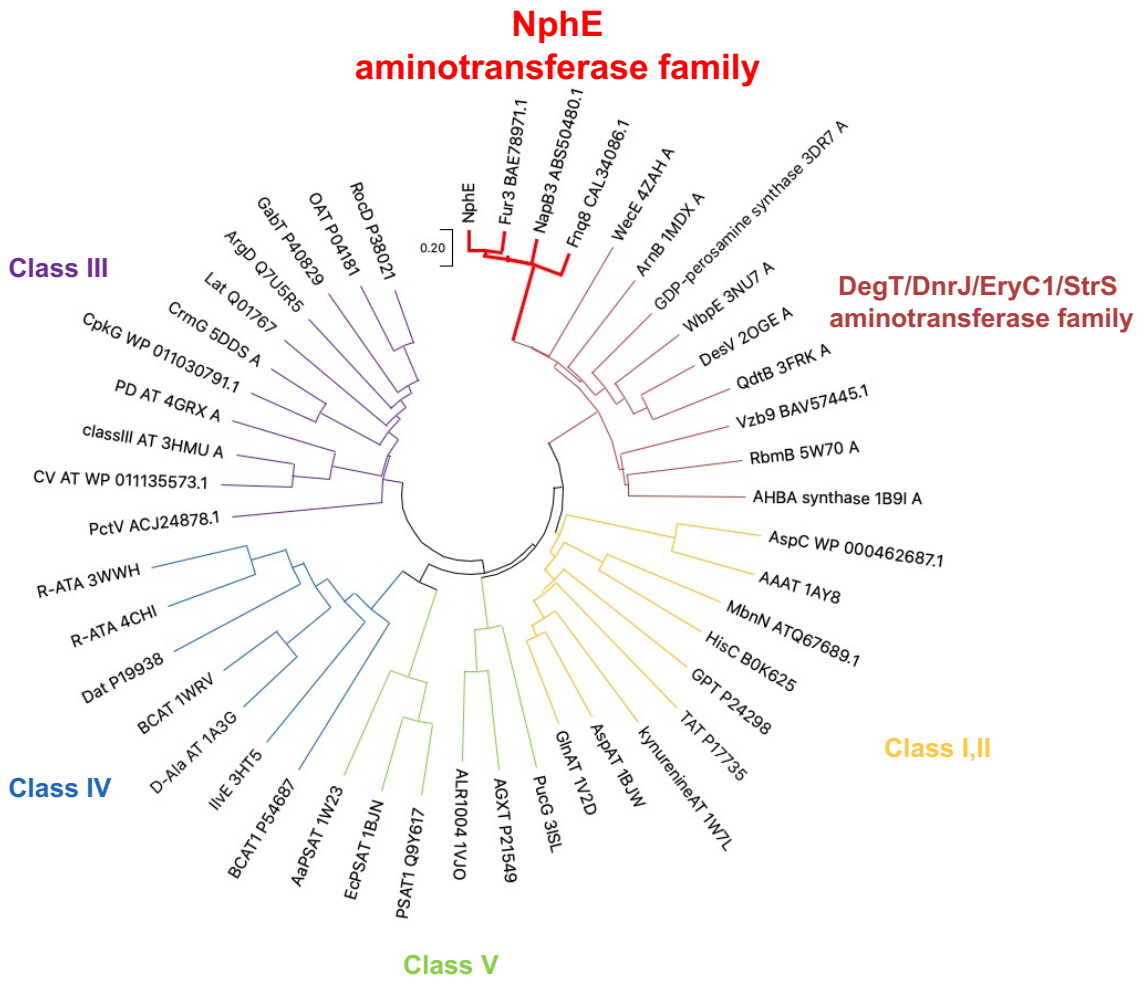

Figure S14. A phylogenetic tree of aminotransferases. The phylogenetic tree was generated with the MEGA X[23] using the Neighbor-joining method. In contrast to other aminotransferases, NphE and its homologs from THN-derived meroterpenoid BGCs form a separate clade. This clade would have branched from DegT/DnrJ/EryC1/StrS aminotransferase family, in which substrates containing a six-membered ring are mainly accepted as amine acceptors for transamination. Therefore, NphE homologs presumably evolved from this family. However, aminotransferases in this family other than NphE homologs are unable to react with O_2. This is consistent with the hypothesis that the evolution of reactions with O_2 may have emerged multiple times because O_2- and PLP-dependent enzymes are distributed in diverse protein families.[24] Thus, we speculate that NphE homologs have evolved to react with O_2 in a convergent evolutionary fashion. PLP is an organic cofactor employed in a wide range of enzymatic reactions, such as transamination, Claisen condensation, β- or γ-elimination, epimerization, decarboxylation, and transaldolation.[25,26] Although PLP-dependent enzymes are estimated to account for ~ 4% of all enzyme activities,[27] only a small number of PLP-dependent enzymes react with molecular oxygen. Thus, our discovery of NphE, oxygen- and PLP-dependent aminotransferase, has expanded the chemical space of PLP-dependent enzymes.

Supplementary References

1. Isogai, S., Nishiyama, M. & Kuzuyama, T. Identification of 8-amino-2,5,7-trihydroxynaphthalene-1,4-dione, a novel intermediate in the biosynthesis of Streptomyces meroterpenoids. *Bioorganic Med. Chem. Lett.* **22**, 5823–5826 (2012).
2. DAIRI, T., Aisaka, K., Katsumata, R. & Hasegawa, M. A Self-defense Gene Homologous to Tetracycline Eflluxing Gene Essential for Antibiotic Production in Streptomyces aureofaciens. *Biosci. Biotech. Biochem* **59**, 1835–1841 (1995).
3. Jez, J. M., Ferrer, J. L., Bowman, M. E., Dixon, R. A. & Noel, J. P. Dissection of malonyl-coenzyme A decarboxylation from polyketide formation in the reaction mechanism of a plant polyketide synthase. *Biochemistry* **39**, 890–902 (2000).
4. Granovsky, A. A. Firefly version 7.1.G. http://classic.chem.msu.su/gran/firefly/index.html (2012).
5. Schmidt, M. W. *et al.* General atomic and molecular electronic structure system. *J. Comput. Chem.* **14**, 1347–1363 (1993).
6. Rausch, C., Lerchner, A., Schiefner, A. & Skerra, A. Crystal structure of the ω-aminotransferase from Paracoccus denitrificans and its phylogenetic relationship with other class III amino- transferases that have biotechnological potential. *Proteins Struct. Funct. Bioinforma.* **81**, 774–787 (2013).
7. Jumper, J. *et al.* Highly accurate protein structure prediction with AlphaFold. *Nat. 2021 5967873* **596**, 583–589 (2021).
8. Schrödinger. PyMOL | www.pymol.org. https://www.pymol.org/pymol.html? (2015).
9. M. J. Frisch, G. W. Trucks, H. B. Schlegel, G. E. Scuseria, M. A. Robb, J. R. C. *et al.* Gaussian 16 Rev. B.01. (2016).
10. Wang, J., Wang, W., Kollman, P. A. & Case, D. A. Automatic atom type and bond type perception in molecular mechanical calculations. *J. Mol. Graph. Model.* **25**, 247–260 (2006).
11. D.A. Case, H.M. Aktulga, K. Belfon, I.Y. Ben-Shalom, S.R. Brozell, D.S. Cerutti, T.E. Cheatham, III, G.A. Cisneros, V.W.D. Cruzeiro, T.A. Darden, R.E. Duke, G. Giambasu, M.K. Gilson, H. Gohlke, A.W. Goetz, R. Harris, S. Izadi, S.A. Izmailov, C. Jin, K. Ka, and P. A. K. Amber 2021. (2021).
12. Maier, J. A. *et al.* ff14SB: Improving the Accuracy of Protein Side Chain and Backbone Parameters from ff99SB. *J. Chem. Theory Comput.* **11**, 3696–3713 (2015).
13. Mobley, D. L., Bayly, C. I., Cooper, M. D., Shirts, M. R. & Dill, K. A. Correction to Small Molecule Hydration Free Energies in Explicit Solvent: An Extensive Test of Fixed-Charge Atomistic Simulations. *J. Chem. Theory Comput.* **11**, 1347 (2015).

14. Jorgensen, W. L., Chandrasekhar, J., Madura, J. D., Impey, R. W. & Klein, M. L. Comparison of simple potential functions for simulating liquid water. *J. Chem. Phys.* **79**, 926–935 (1983).
15. Bussi, G., Donadio, D. & Parrinello, M. Canonical sampling through velocity rescaling. *J. Chem. Phys.* **126**, 014101 (2007).
16. Berendsen, H. J. C., Postma, J. P. M., Van Gunsteren, W. F., Dinola, A. & Haak, J. R. Molecular dynamics with coupling to an external bath. *J. Chem. Phys.* **81**, 3684–3690 (1984).
17. Hess, B., Bekker, H., Berendsen, H. J. C. & Fraaije, J. G. E. M. LINCS: A Linear Constraint Solver for molecular simulations. *J. Comput. Chem.* **18**, 1463–1472 (1997).
18. Hess, B. P-LINCS: A parallel linear constraint solver for molecular simulation. *J. Chem. Theory Comput.* **4**, 116–122 (2008).
19. Darden, T., York, D. & Pedersen, L. Particle mesh Ewald: An N·log(N) method for Ewald sums in large systems. *J. Chem. Phys.* **98**, 10089–10092 (1993).
20. Essmann, U. *et al.* A smooth particle mesh Ewald method. *J. Chem. Phys.* **103**, 8577–8593 (1995).
21. Hess, B., Kutzner, C., Van Der Spoel, D. & Lindahl, E. GRGMACS 4: Algorithms for highly efficient, load-balanced, and scalable molecular simulation. *J. Chem. Theory Comput.* **4**, 435–447 (2008).
22. Hernández-Ortega, A. *et al.* Catalytic Mechanism of Cofactor-Free Dioxygenases and How They Circumvent Spin-Forbidden Oxygenation of Their Substrates. *J. Am. Chem. Soc.* **137**, 7474–7487 (2015).
23. Stecher, G., Tamura, K. & Kumar, S. Molecular Evolutionary Genetics Analysis (MEGA) for macOS. *Mol. Biol. Evol.* **37**, 1237–1239 (2020).
24. Hoffarth, E. R., Rothchild, K. W. & Ryan, K. S. Emergence of oxygen- and pyridoxal phosphate-dependent reactions. *FEBS Journal* vol. 287 1403–1428 (2020).
25. Du, Y. L. & Ryan, K. S. Pyridoxal phosphate-dependent reactions in the biosynthesis of natural products. *Natural Product Reports* vol. 36 430–457 (2019).
26. Liang, J., Han, Q., Tan, Y., Ding, H. & Li, J. Current advances on structure-function relationships of pyridoxal 5'-phosphate-dependent enzymes. *Frontiers in Molecular Biosciences* vol. 6 4 (2019).
27. Percudani, R. & Peracchi, A. A genomic overview of pyridoxal-phosphate-dependent enzymes. *EMBO Reports* vol. 4 850–854 (2003).